Chemistry & Biology, Vol. 9, 839–847, July, 2002, ©2002 Elsevier Science Ltd. All rights reserved. PII S1074-5521(02)00169-2

Sequencing, Modeling, and Selective Inhibition of *Trypanosoma brucei* Hexokinase

Michèle Willson,[1,4] Yves-Henri Sanejouand,[2,4] Jacques Perie,[1] Véronique Hannaert,[3] and Fred Opperdoes[3]
[1]Groupe de Chimie Organique Biologique
Laboratoire Synthèse Physico-Chimie
des Molécules d'Intérêt Biologique
UMR-CNRS-5068
Université Paul Sabatier
31062 Toulouse Cedex
[2]Centre de Recherche Paul Pascal
UPR-CNRS-8641
Université de Bordeaux
33600 Pessac
France
[3]Research Unit for Tropical Diseases
Christian de Duve Institute of Cellular Pathology
and Laboratory of Biochemistry
Université Catholique de Louvain
Brussels
Belgium

Summary

For *Trypanosoma brucei*, a parasite responsible for African sleeping sickness, carbohydrate metabolism is the only source of ATP, and glycolytic enzymes are localized within membrane-bound organelles called glycosomes. Hexokinase, the first enzyme of the glycolytic pathway, was chosen as a target for selective drug design. We have cloned and sequenced the hexokinase gene of *T. brucei*. In parallel, we have synthesized several inhibitors. Kinetic analysis revealed differences in the binding mode of these compounds toward yeast and *T. brucei* hexokinases, while the *m*-bromophenyl glucosamide was found to be selective for *T. brucei*. The modeled structure of *T. brucei* hexokinase-inhibitor complex (using the crystal structure of the *Schistosoma mansoni* hexokinase as a template) allows us to propose a mode of action of this inhibitor for the trypanosome hexokinase and to account for the observed selectivity.

Introduction

Previously, we have studied the inhibition of yeast hexokinase by a series of analogs of glucosamine, a well-known competitive inhibitor of hexokinase [1]. This study was aided by the availability of a crystal structure of a complex between the yeast hexokinase and orthotoluyl-glucosamide (OTG) [2], which provided preliminary information about the mode of binding of a glucose analog to the active site of the enzyme. Using this structure as a scaffold, we have introduced modifications on the substituent at the nitrogen atom of glucosamine and have determined the respective affinities of the resulting compounds for the yeast enzyme. However, since the amino acid sequence of yeast hexokinase was still unknown when its crystal structure in complex with OTG was solved, major uncertainties existed with respect to the actual residues involved in the enzyme's active site. A better understanding of the interactions of a glucose analog with the active-site residues was obtained after a complete rebuilding of the yeast hexokinase structure by using its primary structure when it became available [3]. Moreover, hexokinase undergoes a considerable conformational change during its catalytic cycle [4], and further information on the extent of hinge bending of the enzyme was then obtained by FTIR analysis [5]. In this paper, we extend our studies to the hexokinase of *Trypanosoma brucei*, a blood-dwelling protozoan parasite responsible for human sleeping sickness in Africa. In the blood of the mammalian host, the parasite has access to an unlimited source of glucose, which is maintained at a relatively constant concentration of 5 mM. Glucose is the major substrate for energy metabolism in *T. brucei*, since its mitochondrial metabolism is completely repressed. As a consequence, the Embden-Meyerhoff pathway of glycolysis serves as the sole source of ATP for the parasite [6], which renders the enzymes of the pathway attractive targets for drug intervention. Moreover, the organization of the glycolytic pathway in the trypanosome differs from that in the host in that the first seven enzymes are localized within membrane-bounded organelles called glycosomes [7]. In these highly specialized microbodies, hexokinase, the first enzyme of the glycolytic pathway, catalyses the transfer of the γ phosphoryl group of ATP to a glucose molecule. Almost all glucose 6-phosphate so formed is metabolized by the glycolytic pathway, allowing for the synthesis of ATP, whereas the remainder enters the pentose-phosphate pathway for the synthesis of NADPH and the precursors of nucleic acids. Thus, any inhibition of hexokinase would directly interfere with the formation of both ATP and nucleic acid precursors. The trypanosome enzyme differs from the host enzyme (36%–37% identity with the three human hexokinase isoenzymes) in that it is not inhibited by glucose 6-phosphate. The latter is also twice as large as what has been attributed to a gene duplication that would have taken place during vertebrate evolution [8, 9]. These features render the trypanosome hexokinase an interesting target for selective drug design.

For the design of inhibitors, we reasoned as follows: (1) compounds should be derivatives of glucosamine, to maintain a high degree of similarity with glucose; (2) substitution should only be at the C2 position on the nitrogen atom since, as shown earlier, C6-substituted glucose analogs behaved only as weak inhibitors [10]; (3) in the yeast enzyme the glucose moiety is bound through an amidic bond to an aryl or an alkyl substituent, resulting in its strong binding to the protein; therefore, an aryl substituent was maintained; (4) the length of the aryl substituent should be varied to optimize any contacts with the protein; (5) the substituents on the

[4]Correspondence: willson@chimie.ups-tlse.fr (M.W.), sanejouand@crpp.u-bordeaux.fr (Y.-H.S.)

aromatic ring should be varied with respect to their electron releasing or withdrawing properties; and (6) the meta and ortho positions on the aromatic ring should be varied as well in order to explore the space within the active site by ring rotation.

Here, we present parallel studies of the inhibitory effects by a series of glucosamine derivatives on both the yeast and *T. brucei* hexokinase. Because the three-dimensional (3D) structure of the *T. brucei* hexokinase is not yet known, we have also inferred its structure by first cloning and sequencing its gene and by subsequently modeling its predicted amino acid sequence on the X-ray structure of *Schistosoma mansoni* hexokinase defined with 2.5 Å resolution [11]. From this model of the glucose-hexokinase complex, the position of the inhibitor in the glucose binding site was inferred, and the rebuilt model of the enzyme-inhibitor complex was then compared with the X-ray structure of the complex of yeast hexokinase-OTG as obtained by Steitz [2]. The analysis of different effects in terms of specific interactions between the noncarbohydrate moiety of the inhibitors and the protein has then allowed us to identify the interactions responsible for the selective inhibition of *T. brucei* hexokinase.

Results

Inhibition of Enzymes

Table 1 summarizes the inhibitory effects of glucosamine derivatives on glycosomal hexokinase from *T. brucei* and on hexokinase from yeast (Figure 3). Whereas compounds **1** and **2** show similar effects on both enzymes, substituted derivatives exhibit different patterns. The most pronounced differences are observed with compounds **5** to **8**, which carry an aromatic ring bearing dipoles with external negative charges. A significant selectivity is obtained with compound **8**, since this compound has no effect at 20 mM concentration on the yeast enzyme, whereas its IC50 value for the *T. brucei* enzyme was 0.5 mM.

Kinetic Studies

Table 2 gives the inhibition constants of the different compounds determined for both enzymes and also the extent of ADP formation relative to that of glucose phosphorylation. The inhibition kinetic data with respect to glucose were calculated from Lineweaver-Burk plots (1/v versus 1/glucose) with an intercept on the 1/v axis, at any concentration of the inhibitor. These compounds clearly competed for the substrate glucose by binding at the active site. For the yeast enzyme, compounds **5** and **6** behaved as fully mixed-type inhibitors with two inhibition constants Ki and Kii, the Ki value being lower than the Kii value. For the *T. brucei* enzyme, the inhibition constants for compounds **2**, **3**, and **4** were in the range of the Km value for glucose (110–120 μM); for compounds bearing nitro or bromo substituents on the aromatic ring, the Ki values were considerably lower than the Km for glucose (up to 40 times less for compound **8**).

Since all compounds have an OH group at position 6 of the carbohydrate moiety, they may theoretically serve as pseudosubstrates for the enzyme and be phosphorylated by ATP-Mg. However, we have previously shown that phosphorylation by yeast hexokinase does not occur with this class of inhibitors, although they may induce hydrolysis of ATP by the enzyme [1, 12]. When measuring ADP formation directly by the ATPase assay involving the coupled PyK-LDH reaction, no activity was observed for the *T. brucei* enzyme except with compound **5**, which gave a relatively low rate of ADP produc-

Table 1. Inhibition Values IC50 (mM) for Glucosamine Derivatives on Hexokinase from Yeast and *T. brucei*

R	Compounds	Yeast	*T. brucei*
C6H5	**1**	7	8
o-CH3-C6H4	**2**	8	6
o-NH2-C6H4	**3**	1	4.5
m-NH2-C6H4	**4**	6	1.8
o-NO2-C6H4	**5**	3	0.4
m-NO2-C6H4	**6**	6	2
o-Br-C6H4	**7**	–	3
m-Br-C6H4	**8**	–	0.5
o-I-C6H4	**9**	–	4
CH2Br	**10**	9	3
CH2CH2Br	**11**	7	3

A dash indicates no effect at 20 mM. Each determination is done in triplicate with SD ± 4%.

Table 2. Inhibition Patterns of *T. brucei* and Yeast Hexokinases as Analyzed by Lineweaver-Burk Plots

	Ki (μM)				ADP Formation (% Relative to Glucose-Dependent Activity)	
Compounds	Y		Tb		Y	Tb
1	C	1000 ± 9			5	–
2 (oCH3)	C	1000 ± 8	C	100 ± 1	6	–
3 (oNH2)	C	280 ± 3	C	105 ± 2	34	–
4 (mNH2)	C	200 ± 1	C	114 ± 4	15	–
5 (oNO2)	MT	Ki 500 ± 4 Kii 900 ± 8	C	19 ± 0.5	28	6
6 (mNO2)	MT	Ki 450 ± 1	C	8 ± 0.2	9	–
7 (oBr)			C	25 ± 0.6		–
8 (mBr)			C	2.8 ± 0.1		–
9 (oI)			C	100 ± 1		–
10	C	1100 ± 7	C	70 ± 1	–	–
11	C	1200 ± 6	C	30 ± 0.5	–	–

Tb, *T. brucei*; Y, yeast; C, competitive inhibition; MT, mixed-type inhibition; dash, no ADP formation detected.

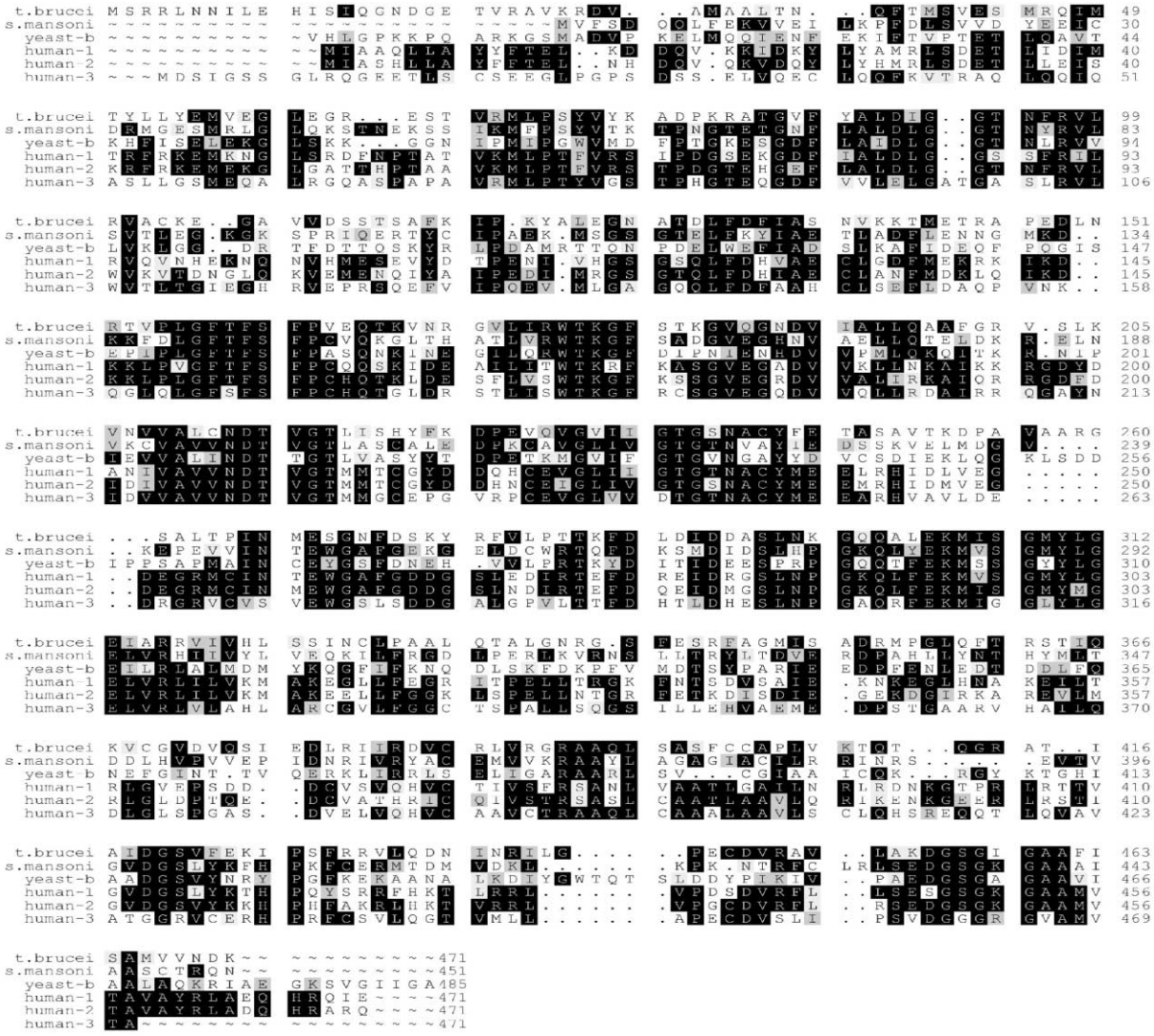

Figure 1. Comparison of the Amino Acid Sequences of the Hexokinase of *T. brucei* with Corresponding Protein of Other Organisms: Yeast, *Schistosoma mansoni*, and Three Human Hexokinase

The sequences were aligned for maximal positional identity using the GCG-Pileup software. The alignment is slightly different from the one used for the modeling. Differences are located in the vicinity of the insertions/deletions, far away from the binding site.

tion. By contrast, compounds **1** to **6** induced a significant rate of ATP hydrolysis by the yeast enzyme.

Cloning and Sequence Determination of the *T. brucei* Hexokinase Gene

Initial attempts to identify the hexokinase gene of *T. brucei* by hybridization with hexokinase genes of some other organisms as probe were unsuccessful, indicating a large divergence between the gene of the trypanosome and that of these different organisms. A different approach was thus taken. The enzyme was purified from *T. brucei* glycosomes, subjected to acid hydrolysis, and some peptide fragments thus obtained were sequenced. The peptide sequences provided us the information to amplify by PCR a genomic fragment that, after sequence analysis, could be used to clone the entire hexokinase gene. The polypeptide encoded by the gene contains 474 amino acids. The calculated molecular mass is 51,189 and the pI is 9.11. This corresponds reasonably well with the measured values of 50,300 Da and pI 10.2, respectively. The amino acid sequence of the *T. brucei* enzyme was aligned with that of some other organisms (Figure 1). Only a very low percentage of sequence identity was observed in the pairwise comparison of the trypanosome hexokinase with each of its counterparts used in this analysis: 30% with yeast hexokinase (isoenzyme B) and 37% with both the *Schistosoma mansoni* enzyme and the human brain hexokinase (isoenzyme I). Our trypanosome gene sequence agrees with those of the various fragments covering only part of the full-length hexokinase gene, as available (September, 2001) in the database of the *T. brucei* genome project.

Modeling Studies with Compound 8

Ten crystallographic structures of hexokinase are presently (September, 2001) available in the Protein Data

Bank. Six of them are mammalian hexokinases, with a molecular weight nearly twice (100,000 M_r) that of *T. brucei* (50,000 M_r). Among the four remaining ones, three are structures of yeast hexokinase, but the most recent one (1IG8) was determined in a free, open form, while the two others were determined when the actual polypeptide sequence was still unknown [13, 14]. Since only 30% of the amino acid sequence as inferred from these crystal structures agreed with the actual residues as deduced later from the gene sequence, these structures would be the wrong starting point for our modeling studies. Therefore, we decided to use the structure of the 50,000 M_r hexokinase from *Schistosoma mansoni* (PDB code 1bdg) [11], which is available at 2.5 Å resolution, while its sequence shares 36% of identical residues with the *T. brucei* sequence (Figure 1). This allows an accurate modeling with standard protocols, especially in the neighborhood of the conserved substrate binding site. Furthermore, this structure is available as a complex with its substrate glucose; the location of the substrate within the active site can be used as a starting point for the positioning of glucose derivatives, as done earlier in the case of the yeast hexokinase [13, 14], an advantage which was exploited in our previous modeling study as well [1]. The *T. brucei* sequence was first modeled on the 3D structure of the *S. mansoni* hexokinase using protein modeling server SWISS MODEL [15–17] developed at Glaxo-SmithKline in Geneva (http://www.expasy.ch). Due to ambiguities in the alignment of the first 59 and the last 4 amino acid residues of the *T. brucei* sequence with that of *S. mansoni*, these residues could not be included in the model. It was assumed that the positioning of the glucose moiety in the active site of the structure of the *S. mansoni* hexokinase-glucose complex and that of the glucose derivatives considered in the present study would be identical. Next, whether the aromatic ring and the peptidic bond are roughly coplanar in the case of *m*-compounds similar to our analogs was checked in the Cambridge Structural Databank, and this was enforced hereafter by adding the corresponding "improper" term in their topological description for the Charmm program [18]. Thus, only two degrees of freedom remained for the positioning of glucose derivative **8** in the active site of the *T. brucei* hexokinase: first, the dihedral angle around the C_2-N_2 bond and second, the *cis* or *trans* location of the *m*-bromine atom (*o*-bromine was not considered here because, due to steric effects, it was expected to disrupt the coplanarity between the aromatic ring and the amidic bond in a manner difficult to predict accurately with empirical forcefields). To determine the importance of the two *cis*/*trans* conformations, each possibility was considered in a separate modeling study which was performed according to the protocol described below.

First, water molecules with bulk water density were added to the *T. brucei* hexokinase-glucose derivative complex, such that they all lay less than 8 Å away from the protein. Then, in order to let the solvent relax, especially within the well-structured and high-density first water shell around the protein [19], the complex was held nearly fixed using harmonic restraints, and a short 10,000 conjugate gradient energy minimization step was performed, followed by a 120 psec molecular dynamics (MD) simulation at T = 300 K. Next, in order to relax the amino acid side chains far away from the binding site, the backbone, the glucose derivative, and the side chains surrounding it (less than 4 Å away) were held fixed, and another 120 psec MD simulation was performed. Finally, in order to relax the aromatic ring of the compound and the side chains in its vicinity, the sugar moiety and the protein backbone were held fixed, as well as all atoms more than 8 Å away from the glucose derivative, a last 320 psec MD simulation was performed, and the average structure obtained over the last 200 psec of this simulation was retained for further analysis.

Tables 3 and 4 and Figure 2 give a detailed analysis of interactions with a listing of Van der Waals contacts and hydrogen bonds between the *m*-bromophenyl part of inhibitor **8** and the *T. brucei* hexokinase from model building.

Table 3. Van der Waals Interactions between the *m*-bromophenyl Part of Inhibitor **8** and *T. brucei*-Hexokinase (from Model Building)

Phenyl Atoms	Contacts < 3 Å	Distances (Å)
C*7	Gln300 (NH)b	2.58
C*2	Gln300 (NH)b	2.64
C*3	Gln300 (NH)b	2.78
C*1	Gln300 (C = O)b	2.87
C*5	Arg176 (NH)	2.74
	Arg176 (N)	2.81
	Gln300 (C = O)b	2.84
C*6	Gln300 (C = O)b	2.75

The numbers and asterisks on carbon atoms are those from the Protein Data Bank for OTG-yeast hexokinase complex (2). b, backbone.

In Vitro Activities

The activity of the different compounds on growing, in vitro cultured *T. brucei* cells was assayed at 5 mM concentration. A significant correlation was found between the affinity of a given compound for *T. brucei* hexokinase and the biological activity on cultures: for nitro and bromo compounds **5**, **6**, and **7** at 5 mM concentration, the percentage of inhibition was 34%, 59%, and 25%, respectively. Again, compound **8** was the most effective, completely inhibiting growth at a dose of 3.6 mM even in the presence of a competing concentration of 5 mM glucose in the cultures, a concentration which is similar to that prevailing in the mammalian bloodstream.

Table 4. Hydrogen Bonds between the *m*-bromophenyl Part of Inhibitor **8** and *T. brucei* Hexokinase's Binding Site (from Model Building)

Donors (X)	Acceptors (Y)	X − Y (Å)
Br	(HN)b-trp177	2.89
Br	(HN)b-Thr178	3.22
C*4	HN-terminal Arg176	2.74
C*4	HN-intra Arg176	2.89
Thr178 − OH	HN − C2	2.32
Gln300 − NH2	O*7	2.18

b, backbone.

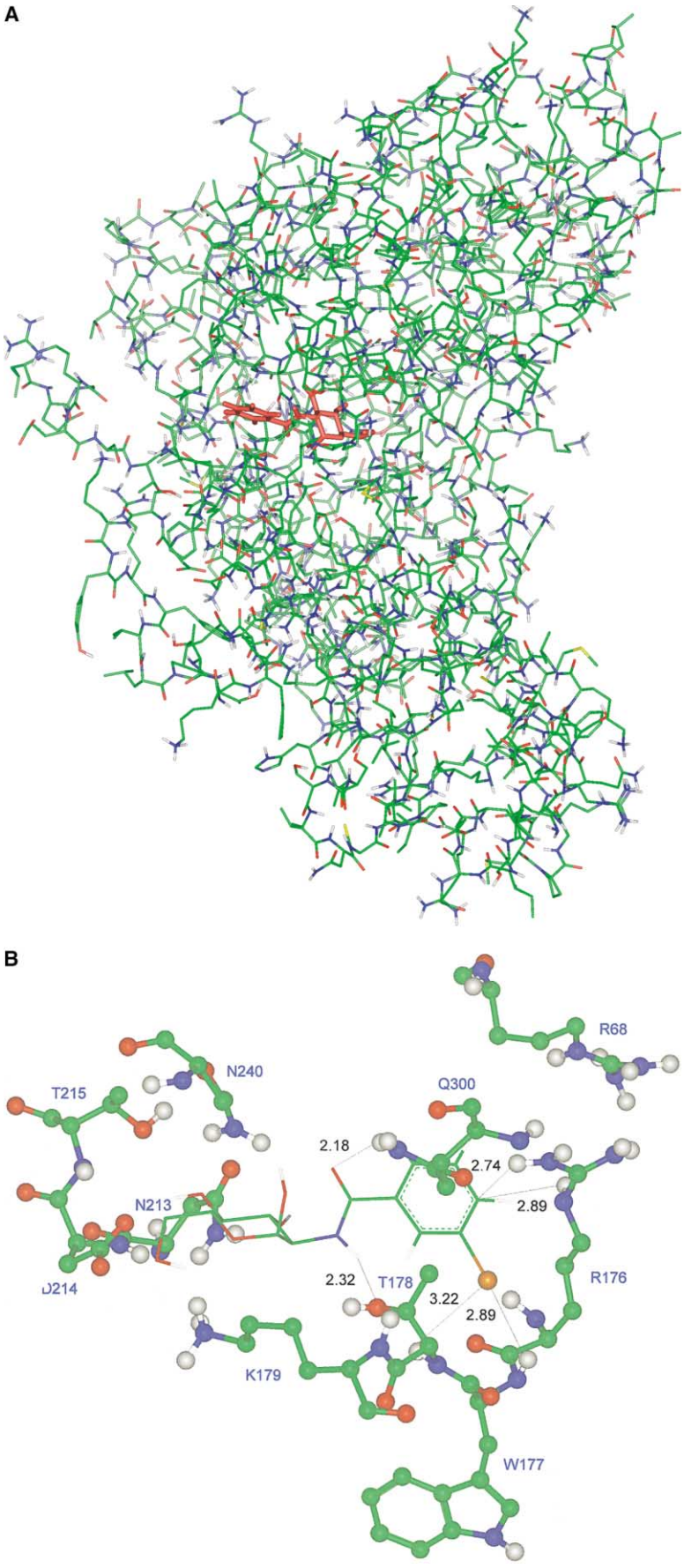

Figure 2. A Model of the *T. brucei* Hexokinase-Glucose Derivative Complex

These figures were made with Molscript.
(A) Predicted 3D structure of hexokinase-inhibitor **8** complex. Green represents the carbon chain and orange-brown represents the inhibitor **8**.
(B) Complex of N-(*m*-bromophenyl) glucosamine **8** in the *Trypanosoma brucei* substrate binding site from model building (ball and stick represents the protein).

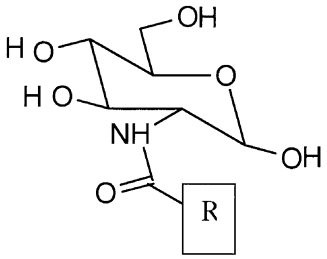

Figure 3. General Structure of the Inhibitors of Hexokinase
R is as described in Table 1.

Discussion

A comparative study in which a set of glucosamine derivatives was tested in activity assays carried out with hexokinase of both yeast and the parasite *T. brucei* allowed us to draw the following conclusions. First, with the exception of reference compound **1**, which contains an unsubstituted ring, the affinities of all compounds were higher for the parasite than for the yeast hexokinase. All compounds behaved as full competitive inhibitors with respect to glucose, with Ki values for *T. brucei* hexokinase ranging from the Km value for glucose (Km 120 μM) to significantly lower values (e.g., nitro and bromo derivatives). Molecules bearing the bulky nitro substituent gave a mixed-type inhibition but only with the yeast hexokinase. Since several glucose-enzyme complexes with different enzymic conformations have been described for the latter enzyme [20], we assume that for our present compounds several inhibitor-hexokinase complexes [1] may exist simultaneously, providing an explanation for the observed mixed-type inhibition. Such different conformations do probably not play a role in the parasite enzyme since only a fully competitive inhibition was observed, suggesting that a single or predominant form of the protein interacts with the inhibitor to give a single EI complex.

Second, brominated molecules are the best inhibitors. Different affinities were found for aliphatic and aromatic inhibitors. The Ki/Km ratio is 0.6 and 0.2 for bromomethyl **10** and bromoethyl **11** glucosamide, respectively, whereas this ratio decreased to 0.02 for the bromophenyl glucosamide **8**. Moreover, the three halogeno-aryl derivatives **7**, **8**, and **9** are selective for the parasite enzyme without any effect on the yeast enzyme.

Third, no ADP formation was detected for any of the inhibitors tested as potential substrates for *T. brucei* hexokinase. In contrast, we have demonstrated previously [5, 12] by using NMR and infrared spectroscopy that yeast hexokinase in the presence of aromatic inhibitors adopts an open conformation that enhances hydrolysis of ATP bound in the active site, whereas aliphatic inhibitors **10** and **11** induce a conformation of the protein similar to the glucose-hexokinase complex. As a consequence, no ATP hydrolysis was observed. The different behavior of the two proteins suggests to us that in the presence of our set of inhibitors, the parasite enzyme always adopts a closed conformation, whereas the yeast enzyme does not always.

Fourth, modeling of the 3D structure of *T. brucei* hexokinase in complex with the *m*-bromine derivative **8** allows us to understand why the latter acts as a selective inhibitor. When the bromine atom is in the *cis* position with respect to the oxygen of the carbonyl group, the average interaction energy between the glucose derivative and the protein is 17 kcal/mole higher than when it is in the *trans* position. This *trans* conformer seems to fit the active site of *T. brucei* hexokinase much better than the *cis* conformer. For this reason, we only consider the *trans* conformer. When the model of the *T. brucei* hexokinase-*m*-bromine derivative complex thus obtained is compared with our previous model of the yeast hexokinase-OTG complex, some clear differences are observed. First, while in both cases the glucose moiety and the amidic bond are roughly perpendicular and in the same relative configuration, the positioning of the aromatic ring is different. In the case of OTG, the aromatic ring and the amidic bond are almost perpendicular, which is likely to be due to the fact that OTG is an ortho-substituted derivative, where steric effects can compete with electronic delocalization. By contrast, in compound **8** the aromatic ring and the amidic bond are coplanar. Second, most of the amino acids found in the direct neighborhood of the two glucose derivatives are highly conserved, but the pattern of interactions is different in both complexes, especially in the vicinity of the aromatic ring. The bromine atom interacts only with the side chains of Arg176, Thr178, and Gln300 (Figure 2), which are all conserved in *T. brucei* and the yeast sequences (Figure 1) (respectively, Arg153, Thr155, and Gln280 in our previous yeast hexokinase model). Note that these three residues are also conserved in the *S. mansoni* hexokinase sequence. Interestingly, Arg176 is replaced by Thr or Ser in the various human isoforms of hexokinase, supporting the underlying hypothesis that some well-chosen *m*-derivative compounds may prove to be specific inhibitors of nonhuman hexokinases. Furthermore, the close proximity of both the terminal and internal NH of Arg176 to the aromatic ring allows a positive charge π electron interaction between the inhibitor and the arginine residue. Such hydrogen bonds are energetically significant in water (5 Kcal/mole) [21] and can account for the high affinity (Ki = 2.8 μM) of compound **8**. Such a tight interaction may also be responsible for bringing the two lobes of the enzyme in close contact, so inducing the closed conformation of the protein. As far as the better affinity of compound **8** for the *T. brucei* enzyme with respect to the yeast one is concerned, given the virtually perfect conservation of most residues lying in the binding site, the only reasonable explanation we found is along the following line: the Cβ atom of Arg58 is 6 Å away from the aromatic ring of compound **8**. Through there is no direct interaction between the end of the side chain of Arg58 and the aromatic ring in our model, such an interaction is geometrically possible. Anyway, it is the only significant difference between the two binding sites in the vicinity of the aromatic ring of compound **8** (in yeast, there is a Pro residue in the corresponding position).

Finally, there exists a clear correlation between the respective affinities of our inhibitors for the *T. brucei* hexokinase and their lethal effect on cells. The LD50 values are in the range of 5–10 mM for inhibitors **5**, **6**,

and **7**. The best inhibitor, **8**, is also the most toxic to the parasite in in vitro culture with a LD100 of 3.6 mM. This dose is relatively high, but this may be due to the fact that glucose, present in the culture medium at a concentration of 5 mM, competes with the drug for the active site of the enzyme. In a separate study, we have measured the affinities of compounds **3** to **8** for the *T. brucei* glucose transporter (THT1) which is responsible for the facilitated diffusion of glucose into the parasite [22]. Our compounds displayed no affinity for this transporter and therefore they most likely enter the trypanosome by passive diffusion rather than by accumulation against a concentration gradient via a mechanism of active transport. Therefore, the intracellular concentration of the inhibitors will most likely not exceed their extracellular concentration.

Our inhibition studies, in combination with the modeling of one of our compounds inside the active site of the *T. brucei* hexokinase, have provided insight into the mode of action of the class of glucosamine analog inhibitors. Moreover, from this work a number of suggestions for improvement of such inhibitors can be proposed. First, we expect more potent inhibitors from the replacement of the bromo substitutent by strongly electron-donating groups, which would ensure the same orientation of the aromatic ring toward Arg176 and would enforce the NH-π electron interaction by increasing the π density. A lethal dose of 3.6 mM of **8** predicts that glucosamine analogs which behave as competitive inhibitors will not be very effective in vivo, because they have to compete with the high concentration of glucose in the blood of the host. In order to become interesting as lead compounds, the affinity of such glucosamine analogs for the enzyme would have to be increased by a 100- to 1000-fold. Second, the problem of low affinity for the glucose binding site and the competition for it by glucose could be overcome by the synthesis of irreversible inhibitors. This would result in a potent mechanism for the inactivation of the enzyme. Such inhibitors should exploit the presence of residue Arg176, which is specific for the *T. brucei* enzyme with respect to human the one, ideally by carrying electrophilic centers that could interact with this residue. Finally, one could envision the synthesis of glucosamine analogs that would enter the cell via a mechanism of active transport. While the trypanosome THT1 transporter is a facilitated diffusion carrier and does not recognize this class of compounds, other trypanosomatids, including *Trypanosoma cruzi* and *Leishmania*, have active carriers for glucose [23] which are able to concentrate glucose against a considerable concentration gradient. Such inhibitors might find their use in the treatment Chagas' disease and Leishmaniasis.

Significance

Owing to the lack of cheap and efficient drugs against sleeping sickness, it is essential to develop new leads based on the inhibition of specific metabolisms for the parasite. Glycolysis meets this requirement since it represents the exclusive source of energy for the parasite in the bloodstream form. Using the 3D structure of yeast hexokinase, it was possible to design a first series of compounds. To obtain selectively criteria for inhibition of the parasite hexokinase, the enzyme was cloned and selective inhibitors could be thus characterized. Their selectivity was rationalized by modeling the inhibitor-enzyme complex based on another parasite hexokinase structure. It is shown that this selectivity is provided by a proper orientation of the aromatic ring attached at the glucose moiety, to make a π-$^{+}NH_3R$ interaction with Arg176. This residue, involved in the binding, only exists in the parasite enzyme. On these grounds, it should now be possible to design more potent irreversible and specific inhibitors exploiting this amino residue as a covalent linker.

Experimental Procedures

Source of Enzymes, Substrates, and Cofactors

Yeast hexokinase, glucose, ATP, NADH, $NADP^{+}$, phospho*enol*pyruvate (PEP), the linking enzymes glucose-6-phosphate dehydrogenase (G6PDH), pyruvate kinase (PyK), and lactate dehydrogenase (LDH) were purchased from Roche (Germany). The hexokinase from *T. brucei* was purified as described by Misset et al. [8].

Synthesis of Inhibitors

The pure compounds were identified by spectrometric analysis on apparatus of the Institute of Molecular Chemistry Paul Sabatier (ICMPS-IR1744). IR spectra were recorded on a Perkin-Elmer FTIR 1610 spectrometer, 1H and 13C NMR spectra were run on a Bruker 250MHZ FT apparatus, and mass spectra were determined on a Nemag R10-10.

The synthesis of compounds **1–7** was achieved as described in Willson et al. [1]. For compounds **8–11**, the general procedure for their synthesis was a coupling reaction between the unprotected D-glucosamine hydrochloride and the appropriate *p*-nitro-phenyl esters [24] under stoichiometric conditions at room temperature in dimethylsulfoxide (DMSO). In the preceding step, the *p*-nitrophenyl esters were prepared by reaction of *p*-nitrophenol with the halide of carboxylic acids : 3-bromobenzoyl chloride, 2-iodobenzoyl chloride, bromoacetyl bromide, and 3-bromopropionyl chloride. Before the coupling reaction, the glucosamine hydrochloride was neutralized with a tertiary organic base (triethylamine) in DMSO. The products were subsequently extracted from the DMSO solution by precipitation with dichloromethane. They were purified by recrystallization from a large volume of ethanol. The atom numbering used in Tables 3 and 4 is as that in the Protein Data Bank for the OTG-yeast hexokinase complex [2].

***N-(*m*-bromobenzoyl)-D-glucosamine** 8*

Yield = 60%. TLC (eluent ethanol) Rf = 0.75. IR (pellet) ν cm^{-1} 1632 (C = O). ^{1}H NMR (DMSO-D6); δ (ppm) 6.75 (d, NH, J = 6.3Hz), 5.74 (C1H, J = 4.5Hz). ^{13}C NMR (DMSO-D6); δ (ppm) (α and β forms): 56.3-58.1 (C2), 61.4 (C6), 70.10-71.0 (C3), 71.2-74.1 (C4), 72.1-76.9 (C5), 91.3-96.3 (C1), 128.1 (C*4), 118.0 (C*6), 130.2-129.3 (C*3-C*1), 131.6-132.0 (C*5), 134.4-134.9 (C*2), 167.3-167.5 (C*7). Mass: (FAB), MH^{+}, 361; MNa^{+}, 384.

***N-(*o*-iodobenzoyl)-D-glucosamine** 9*

Yield = 72%. TLC (eluent ethanol) Rf = 0.85. IR (pellet) ν cm^{-1} 1672 (C = O). ^{1}H NMR (DMSO-D6); δ (ppm) 6.62 (d, NH, J = 6.1Hz), 5.80 (C1H, J = 4.3Hz). ^{13}C NMR (DMSO-D6); δ (ppm) (α and β forms): 59.3-56.5 (C2), 62.9 (C6), 72.5 (C3), 72.4-76.0 (C4), 72.2-76.1 (C5), 92.5-97.0 (C1), 92.5 (C*1), 129.1-129.3 (C*4), 129.3-129.4 (C*3), 132.0 (C*6), 140.8-141.0 (C*5), 144.1 (C*2), 172.6 (C*7). Mass: (DCI), MH^{+}, 408; MNH_4^{+}, 425.

***N-(bromo-acetyl)-D-glucosamine)** 10*

Yield = 48%. TLC (eluent ethanol) Rf = 0.60. IR (pellet) ν cm^{-1} 1712 (C = O). ^{1}H NMR (DMSO-D6); δ (ppm) 6.82 (d, NH, J = 6.2Hz), 4.25 (s, CH2Br). ^{13}C NMR (DMSO-D6); δ (ppm) (α and β forms): 44.8-44.9 (C8), 57.0-59.7 (C2), 63.1-63.3 (C6), 72.4-72.6 (C3), 73.2-74.1 (C4), 76.1-78.5 (C5), 93.2-97.1 (C1), 172.6-172.9 (C7). Mass (DCI), MH^{+}, 301; MNH4^{+}, 317.

N-(bromo-propionyl)-D-glucosamine 11

Yield = 54%. TLC (eluent ethanol) Rf = 0.60. IR (pellet) ν cm^{-1} 1720 (C = O). ^1H NMR (DMSO-D6); δ (ppm) 6.78 (d, NH, J = 5.9Hz), 2.32 (t, CH2 CO), 3.10 (t, CH2Br). ^{13}C NMR (DMSO-D6); δ (ppm) (α and β forms): 30.1-30.3 (C8), 40.9-41.4 (C9), 56.6-59.3 (C2), 63.0-63.22 (C6), 72.3-72.5 (C3), 73.1-76.2 (C4), 76.3-78.4 (C5), 93.3-97.3 (C1), 176.1-176.4 (C7). Mass (DCI), MH^+ 314; $MNH4^+$ 331.

Cloning and Sequencing of *T. brucei* Hexokinase Gene

Peptides of purified glycosomal hexokinase were prepared by acid hydrolysis [25] and purified. Seven of the peptides were sequenced by classical automated Edman degradation, but only two could be aligned with amino acid sequences of hexokinases from various organisms (peptide 1, LNRTVPLGFTFSFP?VEQTKVNRGVLIRFTK H?FS?L?; peptide 2, TVGTLISHYFKAI?KEGAV). Based on these sequences, a sense primer 5′-CGCGGATCCGTNGARCARACNAARG TNAA-3′ and an antisense primer 5′-CGCGGATCCTCYTTDATNG CYTTRAARTA-3′ containing BamH1 sites (underlined) were designed and used for PCR amplification with purified genomic DNA as template. Several DNA fragments were obtained. After sequencing, one of the clones, with an insert of approximately 200 bp (corresponding to residues 164–226 in the *T. brucei* amino acid sequence), appeared to have hexokinase-specific motifs and was used to screen a genomic library of *T. brucei* in *Escherichia coli* prepared with the vector λGEM11 (Promega, USA) as described previously [26]. Plaques of positive clones were processed, the DNA was purified, and an appropriate restriction fragment containing the hexokinase gene was subcloned in the phagemid pTZ18R (Amersham-Pharmacia Biotech, Sweden). DNA sequence determination was performed on both strands by the chain-termination method using the T7 DNA polymerase kit of Amersham-Pharmacia Biotech with double-stranded DNA as template, [^{35}S]dATP (PerkinElmer Life Sciences, USA), and specific, custom-made oligonucleotides (Invitrogen/Life Technologies, UK) as primers.

Assay of Enzyme Activities

The phosphotransferase activity and the consumption of ATP were measured spectrophotometrically by reduction of $NADP^+$ or oxidation of NADH in the coupled assays shown in the following equations.

Method A:

$$G + \text{ATP-Mg} \xrightarrow{HK} G6P + (\text{ADP-Mg}) + NADP \xrightarrow{G6PDH} NADPH + \text{phospho-gluconolactone}$$

Method B:

$$\text{ATP-Mg} + G \xrightarrow{HK} (G6P) + \text{ADP-Mg} + PEP \xrightarrow{PyK} \text{ATP-Mg} + \text{lactate} + NAD \xrightarrow{LDH} NADH + \text{pyruvate}$$

Kinetic Studies

The inhibition of hexokinase by compounds was measured by assaying the enzyme activity in the direction of NADPH and NADH formation; the concentration of the cofactors was calculated from their absorbance using an $\epsilon_{340} = 6.22\ mM^{-1}cm^{-1}$. All reactions were carried out at 25°C, and the formation of NADH or NAD^+ at 340 nm was measured with a PerkinElmer spectrophotometer equipped with a kinetic accessory unit. The activities of the compounds on hexokinase were measured after 5 min of preincubation of the enzyme with the compound in the assay buffer, followed by addition of a mixture to start the reaction.

For the phosphotransferase activity (method A), the reaction mixture (1 mL) contained 0.1 M triethanolamine hydrochloride buffer (pH 7.6), 1 mM EDTA, 0.64 mM $NADP^+$, 0.66 mM ATP, 10 mM $MgCl_2$, 10 mM glucose, and 5 μg G6PDH (0.7 unit).

For following the formation of ADP-Mg (method B), the reaction mixture (1 mL) contained 0.1M triethanolamine hydrochloride buffer (pH 7.6), 1 mM EDTA, 0.42 mM NADH, 2.5 mM PEP, 0.66 mM ATP, 10 mM $MgCl_2$, PyK/LDH (1.12 unit).

Possible interference of the inhibitors with the absorbance of NADPH or NADH was verified by running blank reactions without enzyme. The remaining activity was calculated from comparison with control experiments in which the inhibitor was replaced by the same amount of the solvent DMSO; at a solvent concentration in the buffer below 10%, no significant effect on the enzyme activity was observed. The concentration of inhibitor required for 50% inhibition (IC50) was calculated from at least 5 inhibitor concentrations; they were tested with substrates present at saturating concentrations. The type of inhibition and the inhibition constant (Ki) were determined from Lineweaver-Burk plots. The inhibition with respect to glucose was studied at three different concentrations of glucose (100 μM, 200 μM, and 300 μM) at a saturating concentration of ATP (0.66 mM). To determine whether the compounds could be phosphorylated by the enzyme at the expense of ATP, we measured the amount of ADP formed in the presence of 10 mM of the inhibitor as a substrate, without glucose, relative to the amount of ADP produced with only 10 mM of glucose.

Molecular Modeling and Molecular Dynamics

The Charmm program [18], version 24, was used in order to perform all structural optimizations. Nonbonded interactions were calculated using a 7.5 Å cutoff, a shifting function for electrostatics as well as a switching function for Lennard-Jones interactions, within a 6.5–7.5 Å distance range. All distances between bonded atoms were constrained, using the SHAKE algorithm, allowing for the use of a 0.002 psec time step in order to integrate the equations of atomic motion. The temperature was controlled through the coupling of the system to an external thermal bath, mimicked by Langevin forces acting on all atoms, with a 1.5 ps^{-1} friction constant.

Measurement of Antitrypanosomal Activity In Vitro

T. brucei bloodstream forms were cultured in vitro in a modified Iscove's medium containing 10% heat-inactivated fetal calf serum (HI-FCS) and bloodstream form supporting factors 0.05 mM bathocuproine sulfonate, 1.5 mM L-cysteine, 1 mM hypoxanthine, 0.2 mM 2-mercaptoethanol, 1 mM sodium pyruvate, 0.16 mM thymidine (HMI 9) [27]. Cells were incubated in a humidified atmosphere containing 5% CO_2 at 37°C. The effect of the compounds was tested essentially as described by Freiburghaus et al. [28]. Compounds were initially dissolved in DMSO and/or water and diluted with the medium. Aqueous solutions were sterilized by filtration before being diluted. The highest concentration of DMSO after serial dilution with complete culture medium was 1%. Each compound was tested in duplicate in 96-well microtiter plates in 3-fold serial dilutions. Fifty microliters of a cell suspension in complete medium (5×10^4cells/ml) was added to each well. After incubation for 72 hr, each plate was examined with an inverted microscope to determine the minimum inhibitory concentration (MIC), which is the concentration at which no cell with a normal morphology and/or motility is found in comparison to the control. Afterwards, Alamar Blue was added into each well to reach a final concentration of 5%, and the plates were incubated for 4 hr before viability was determined using a cytofluorimeter (Millipore Cytofluor 2300, Millipore, USA). The excitation wavelength was 530 nm, and the emission wavelength was 590 nm. Control wells without inhibitor were included as well as blanks without cells.

Acknowledgments

This research was financially supported by the European-Union (contrat IC18-CT970220) and GDR-CNRS-GGA 2177, which are both fully acknowledged. We are grateful to Mr. Joris Van Roy (ICP, Brussels) for his assistance in the enzyme purification, Mme. Christiane Vidal for assistance in the modeling study, and Paul A.M. Michels for critical reading of the manuscript.

Received: October 24, 2001
Revised: May 21, 2002
Accepted: June 9, 2002

References

1. Willson, M., Alric, I., Périé, J., and Sanejouand, Y.H. (1997). Yeast hexokinase inhibitors designed from the 3-D enzyme structure rebuilding. J. Enzyme Inhib. *12*, 101–121.
2. Steitz, T.A., Anderson, W.F., Fletterick, R.J., and Anderson, C.M. (1977). High resolution crystal structure of yeast hexokinase complex with substrates, activators and inhibitors. J. Biol. Chem. *252*, 945–963.
3. Stachelek, C., Stachelek, J., Swan, J., Boistein, D., and Konigsberg, W. (1986). Identification, cloning and sequence determination of genes specifying hexokinase A and B from Yeast. Nucleic Acids Res. *14*, 945–963.
4. Bennett, W.S., and Steitz, T.A. (1978). Glucose induced conformational change in yeast hexokinase. Proc. Natl. Acad. Sci. USA *75*, 4848–4859.
5. Trinquier, M., Boisdon, M.T., Périé, J., and Willson, M. (1998). A Fourier transform infrared spectroscopic study of yeast hexokinase:conformational changes under interaction with substrates and inhibitors. Spectrochemica Acta Part A *54*, 367–373.
6. Opperdoes, F.R., and Borst, P. (1977). Localization of nine glycolytic enzymes in a microbody-like organelle in *Trypanosoma brucei*:the glycosome. FEBS Lett. *80*, 360–364.
7. Opperdoes, F.R. (1987). Comparmentation in trypanosomes. Annu. Rev. Microbiol. *41*, 127–151.
8. Misset, O., and Opperdoes, F.R. (1984). Simultaneous purification of hexokinase, class-1 fructose-bisphosphate aldolase, triosephosphate isomerase and phosphoglycerate kinase from *Trypanosoma brucei*. Eur. J. Biochem. *144*, 475–483.
9. Misset, O., Bos, O.J.M., and Opperdoes, F.R. (1986). Glycolytic enzymes of *Trypanosoma brucei*. Simultaneous purification, intraglycosomal concentrations and physical properties. Eur. J. Biochem. *157*, 441–453.
10. Alric, I., Willson, M., and Périé, J. (1991). Synthèse d'analogues de glucose-6-phosphate, inhibiteurs potentiels d'hexokinase. Phosphorus and Sulfur *56*, 71–80.
11. Mulichak, A.M., Wilson, J.E., Padmanabhan, K., and Garavito, R.M. (1998). The structure of mammalian hexokinase-1. Nat. Struct. Biol. *5*, 555–560.
12. Willson, M., and Périé, J. (1999). Inhibition of yeast hexokinase: a kinetic and phosphorus nuclear magnetic resonance study. Spectrochemica Acta Part A *55*, 911–917.
13. Bennett, W.S., and Steitz, T.A. (1980). Structure of a complex between yeast hexokinase and glucose. I Structure determination and refinement at 3.5Å. J. Mol. Biol. *140*, 183–209.
14. Bennett, W.S., and Steitz, T.A. (1980). Structure of a complex between yeast hexokinase and glucose. II Detailed comparison of conformation and active site configuration with the native hexokinase B monomer and dimer. J. Mol. Biol. *140*, 211–230.
15. Peitsch, M.C. (1995). Protein modeling by E-mail. Biotechnology *13*, 658–660.
16. Peitsch, M.C. (1996). Promod and swiss model: internet-based tools for automated comparative protein modeling. Biochem. Soc. Trans. *24*, 274–279.
17. Guex, N., and Peitsch, M.C. (1997). Swiss-model and swiss-pdb viewer: an environment for comparative protein modeling. Electrophoresis *18*, 2714–2723.
18. Brooks, B.R., Bruccoleri, R.E., Olafson, B.D., States, D.J., Swaminathan, S., and Karplus, M. (1983). A program for macromolecular energy, minimization and dynamics calculations. J. Comput. Chem. *4*, 187–217.
19. Alary, F., Durup, J., and Sanejouand, Y.H. (1993). Molecular Dynamic study of the hydratation structure of an antigene-antibody complex. J. Phys. Chem. *97*, 13864–13876.
20. Rose, I.A. (1995). Partition analysis: detecting enzyme reaction cycle intermediates. Methods Enzymol. *249*, 315–340.
21. Gallivan, J.P., and Dougherty, D.A. (2000). A computational study of cation-π interaction vs salt bridges in aqueous media: implication for protein engeneering. J. Am. Chem. Soc. *122*, 870–874.
22. Game, S., Holman, G., and Eisenthal, R. (1986). Sugar transport in *Trypanosoma brucei*:a suitable kinetic. FEBS Lett. *194*, 126–130.
23. Tetaud, E., Barrett, M., Bringaud, F., and Baltz, T. (1997). Kinetoplastides glucose transporters. Biochem. J. *325*, 569–580.
24. Mukherjee, H., and Pal, R.P. (1970). N-acylation of D-glucosamine by a new method. J. Org. Chem. *35*, 2042–2044.
25. Allen, G. (1989). Laboratory Techniques in Biochemistry and Molecular Biology, Volume 9, R.H. Burdon and P.H. Van Knippenberg, eds. (Amsterdam: Elsevier/North-Holland).
26. Michels, P.A.M., Marchand, M., Kohl, L., Allert, S., Wierenga, R.K., and Opperdoes, F.R. (1991). The cytosolic and glycosomal isoenzyme of glyceraldehyde-3-phosphate dehydrogenase in *Trypanosoma brucei* have a distant evolutionary relationship. Eur. J. Biochem. *198*, 421–428.
27. Hirumi, H., and Hirumi, K. (1994). Axemic culture of african trypanosome bloodstream forms. Parasitol. Today *10*, 80–84.
28. Freiburghaus, F., Kaminsky, R., Nkunya, M.H.H., and Brun, R. (1996). Evaluation of african medicinal plants for their *in vitro* trypanocidal activity. J. Ethnopharmacol. *55*, 1–11.

Accession Numbers

Nucleotide sequence data reported in this paper are available in the EMBL, GenBank, and DDJB databases under the accession number AJ345044, *Trypanosoma brucei* HK gene for hexokinase.